Supplement of Earth Surf. Dynam., 13, 349–363, 2025
https://doi.org/10.5194/esurf-13-349-2025-supplement

Supplement of

Influence of alluvial slope on avulsion in river deltas

Octria A. Prasojo et al.

Correspondence to: Octria A. Prasojo (octria.prasojo@glasgow.ac.uk)

Contents of this file

Figures S1 to S6
Table S1 to S2
Video S1

Figure S1. Density plot showing distribution of delta topset slope value.

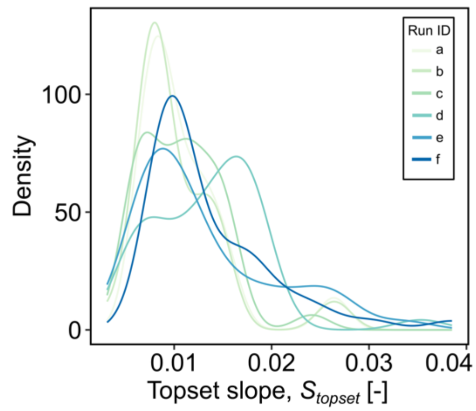

Figure S2. Run f reaching the model's boundary.

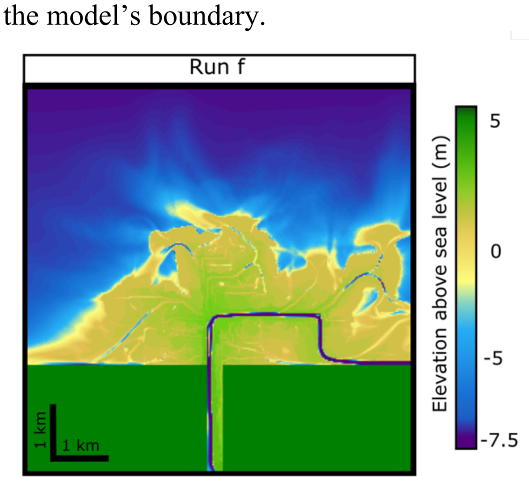

Figure S3. Boxplots showing distribution of avulsion timescale ($T_{a\ \mathrm{empirical}}$) observed in the model.

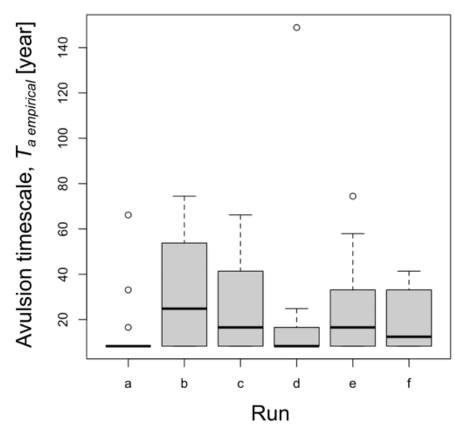

Figure S4. Time series plot of topset slope (a), delta lobe width (b) and avulsion length (c) observed in our model

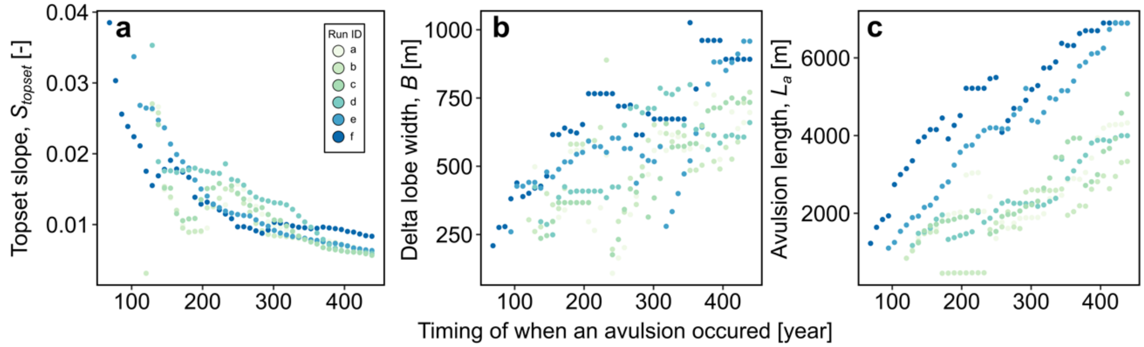

Figure S5. Correlation between avulsion timescale produced by our model ($T_{a\ empirical}$), analytical model ($T_{a\ H^* = 1.4}$, $T_{a\ H^* = 0.5}$, $T_{a\ H^* = 0.2}$), natural deltas ($T_{a\ natural}$) and relative sea-level rise (*RSLR*) plotted on semi-log plot.

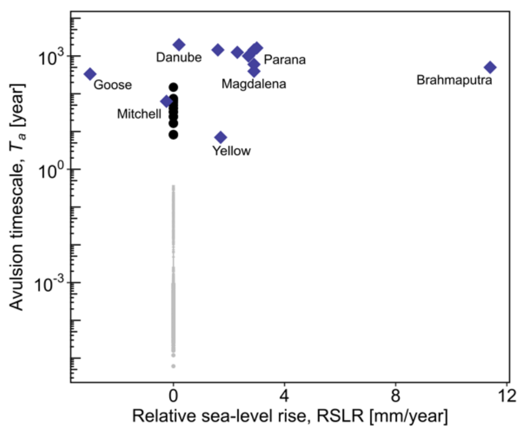

Figure S6. Plot between avulsion length (L_a) and backwater length produced from our model scenarios (L_b) along with linear regression line for each scenario.

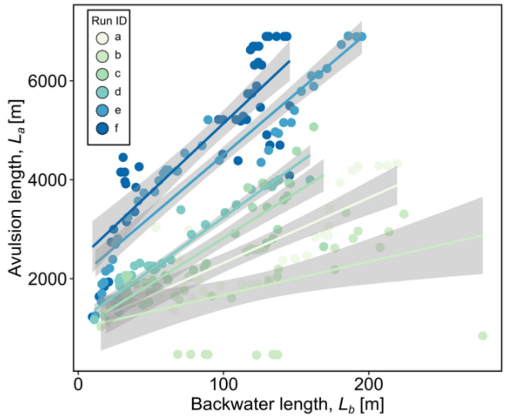

Run ID
a
b
c
d
e
f
6000
4000
2000
0
100
200
Avulsion length, L_a [m]
Backwater length, L_b [m]

Table S1. Measured morphometric variables and avulsion timescales from our model (attached as Excel file).

Table S2. River delta avulsion timescales from natural and laboratory experiment collected from the literature.

ID	h_c [m]	B_c [m]	Q_s [km^3/y]	H_b [m]	L_a [km]	$\boldsymbol{\sigma}$[1] [mm/y]	B [km]	N [-]	v_a [m/yr]	H [m]	S_{topset} [-]	T_a [year]	Source
Parana	11.8	1270	0.03	40	210	3	50.8	4	0.005		0.000053	1633	Chadwick et al., 2020; Prasojo et al., 2022
Danube	6.3	1250	0.025	50	95	0.2	50	4	0.0025		0.0000119	1991	Chadwick et al., 2020; Prasojo et al., 2022
Nile	16.2	240	0.045	120	210	4.5	9.6	4			0.0000686		Chadwick et al., 2020; Prasojo et al., 2022
Mississippi	21	650	0.15	80	490	2.3	26	4	0.01		0.0000602	1250	Chadwick et al., 2020; Prasojo et al., 2022
Assiniboine	4.2	100	0.00036	7	12		4	4	0.0014	4.2	0.0005	1000	Chadwick et al., 2020; Jerolmack & Mohrig, 2007; Prasojo et al., 2022
Rhine-Meuse	5	700	0.0012	18	51	1.6	28	4	0.0016		0.00011	1450	Chadwick et al., 2020; Prasojo et al., 2022
Magdalena	6	1100	0.083	200	67	2.9	44	4	0.0038	6	0.0000512	394.7	Chadwick et al., 2020; Jerolmack & Mohrig, 2007; Prasojo et al., 2022
Orinoco	8	2000	0.057	110	78	2.7	80	4	0.0021		0.0000413	1000	Chadwick et al., 2020; Prasojo et al., 2022
Mid-Amazon	12	3000	0.45	50	404	2.9	120	4	0.005	12	0.00003	600	Chadwick et al., 2020; Jerolmack & Mohrig, 2007; Prasojo et al., 2022
Upper-Rhone	5.4	377	0.012	70		2.9	15.08	4	0.002	5.9	0.000382	1450	Chadwick et al., 2020; Prasojo et al., 2022
Yellow	3.5	500	0.42	30	31	1.7	20	4	0.1		0.0000965	7	Chadwick et al., 2020; Prasojo et al., 2022
Brahmaputra	7	3300	0.2	80		11.4	132	4	0.02	7	0.0001	500	Chadwick et al., 2020; Prasojo et al., 2022
Goose	2	100	0.00013	10		-3	4	4	0.00198			333	Chadwick et al., 2020; Prasojo et al., 2022
Mitchell	7	100	0.0011	15		-0.25	4	4				63	Chadwick et al., 2020; Prasojo et al., 2022
Trinity	5	200	0.0023	8		4.2	8	4	0.0011				Chadwick et al., 2020; Prasojo et al., 2022

Okavango				0.00019	100	Jerolmack & Mohrig, 2007; Prasojo et al., 2022
Gilbert	7	0.0007	6	0.00006	1224.4898	Jerolmack & Mohrig, 2007; Prasojo et al., 2022
Suwanee	3	0.001	3	0.00007	1000	Jerolmack & Mohrig, 2007; Prasojo et al., 2022
McArthur	2	0.0005	5	0.00006	5000	Jerolmack & Mohrig, 2007; Prasojo et al., 2022
Emerald Lake Fan	1	3.65	0.3	0.035	0.08	Jerolmack & Mohrig, 2007; Prasojo et al., 2022
Rolling Stone Fan	1	0.63	0.1	0.0064	0.16	Jerolmack & Mohrig, 2007; Prasojo et al., 2022
XES 1999 Lab Fan Run 1, Stage 3	9	17.52	0	0.06	0.00005	Jerolmack & Mohrig, 2007; Prasojo et al., 2022

[1]relative sea-level rise rate as the sum of the coastal subsidence rate and eustatic sea level rise rate. Please refer to the main text for the abbreviations on the header.

Video S1. Timelapse of bed level change, sediment concentration of cohesive and non-cohesive grain size throughout the simulation.